Limit Cycling Behavior of a Hybrid System: Application to Percussive Drilling

Depouhon Alexandre[a,b], Detournay Emmanuel[b,c], and Denoël Vincent[a]

[a] *ArGEnCo, Université de Liège, Belgium*

[b] *Department of Civil Engineering, University of Minnesota, MN, USA*

[c] *CSIRO Earth Science and Resource Engineering, Australia*

1 Introduction and Mathematical Modeling

Percussive drilling has nowadays become the reference technology for drilling hard geological formations and, as such, is ubiquitous in the exploitation of earth resources. Despite this extensive use, the technological process is not fully understood and suffers a lack of proper modeling framework. In particular, there is no explanation to the existence of optimal control configurations that maximize the penetration rate of the tool for a given rock formation [2].

Depouhon et al. [4] have proposed a simple model for the study of the process and the identification of optimal control parameters based on the numerical analysis of its steady-state response or limit cycling behavior. They model the bit dynamics by a 1 degree-of-freedom oscillator impulsively loaded in the field of gravity and subject to a bilinear bit/rock interaction (BRI) law. This model, presented in Figure 1-(a), comprises three types of forces: (i) λ_S a static force representing the conjugated effect of gravity and thrust; (ii) $\delta\lambda_\psi = \sum_{i\in\mathbb{N}} \delta\left(\tau - i\psi - \tau_s\right)$ a periodic impulsive force of constant dimensionless unit impulsion, period ψ and time shift $0 \leq \tau_s < \psi$, leading to activations at times $\tau_i = i\psi + \tau_s,\ i \in \mathbb{N}$; and (iii) φ_R the reaction force of the rock on the bit that follows the bilinear model depicted in Figure 1-(b). The non-smooth nature of the latter leads to the definition of three drilling phases: (i) *forward contact* (FC), the bit motion is downwards while there is contact between the bit and the rock; (ii) *backward contact* (BC), contact is established but the bit is moving upwards;

The financial supports of the Commonwealth Scientific and Industrial Organisation (CSIRO) and of Itasca International Ltd. are gratefully acknowledged.

and (iii) *free flight* (FF), the bit is flying off the hole bottom, the force exerted by the rock is zero.

Between two percussive activations, bit motion is ruled by the dynamics of one of these regimes. Referring to the dimensionless penetration while drilling by θ, the governing equation for each regime reads

$$\begin{aligned} FC\!: &\qquad \bar{\bar{\theta}} + \theta = \lambda_S, \\ BC\!: &\qquad \bar{\bar{\theta}} + \gamma\theta = \lambda_S + (\gamma - 1)\,\theta_p, \\ FF\!: &\qquad \bar{\bar{\theta}} = \lambda_S. \end{aligned} \tag{1}$$

In the above equations, the overhead bar denotes differentiation with respect to the dimensionless time while $\gamma > 1$ represents the unloading slope of the BRI law and θ_p defines the peak penetration along the drilling cycle; see Figure 1-(b). Given the impulsive nature of the loading, at each activation, the bit velocity jumps by an amount $0 < \eta \leq 1$

$$\bar{\theta}\left(\tau_i^+\right) = \bar{\theta}\left(\tau_i^-\right) + \eta, \quad i \in \mathbb{N}. \tag{2}$$

Coefficient η characterizes the efficiency of the momentum transfer between the hammer and the bit. It is related to the contact conditions at the bit/rock interface as well as to the geometries of the hammer and the bit, and embodies wave propagation effects that can be seen as instantaneous on the timescale of bit motion. We assume a perfect transfer in this preliminary study and set $\eta = 1$.

The transition conditions for the passage of one drilling phase to the other are given by the locations of the non-smooth points along the drilling cycle and by the occurrence of activation. While the former category of events is state-dependent, the latter is time-dependent. They read

$$\begin{aligned} &FC{\to}BC : \bar{\theta}\,(\tau) = 0, \quad BC{\to}FF : \theta\,(\tau) = \frac{\gamma - 1}{\gamma}\theta_p, \\ &FF{\to}FC : \theta\,(\tau) = \theta_u, \quad BC{\to}FC : \bar{\theta}\left(\tau_i^+\right) \cdot \bar{\theta}\left(\tau_i^-\right) < 0, \end{aligned} \tag{3}$$

where θ_u corresponds to the penetration at the end of the drilling cycle, when the bit either enters the FF phase or the FC one upon exiting the BC phase. The penetration is reset to zero or to the residual penetration $\theta_\ell = (1 - \gamma)\theta_p + \gamma\theta_u$ at $FF{\to}FC$ and $BC{\to}FC$ transitions respectively.

Variables θ_ℓ, θ_p and θ_u are of a peculiar type. They are *history variables*. They capture the past history of BRI law at the points of non-smoothness along the drilling cycle: the lower, peak and upper points; see Figure 1-(b). As such, they do evolve in a stepwise manner, their update taking place at the instant the system goes through the corresponding point of the interface law.

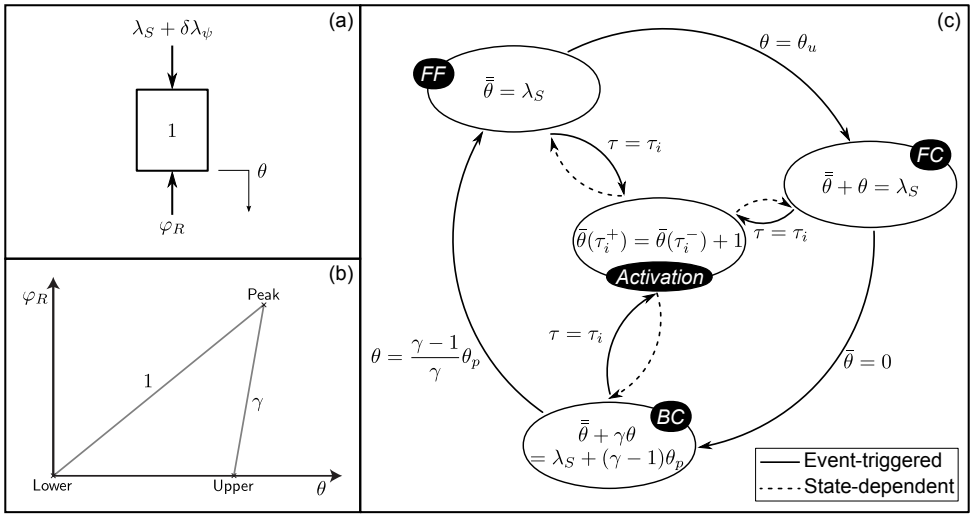

Figure 1: Panel (a) shows the dimensionless model proposed in [4] with the BRI law depicted in panel (b). Panel (c) illustrates the hybrid and sequential nature of the governing equations.

The handling of history variables in the definition of initial conditions and the assessment of limit cycles properties requires specific care. This paper addresses these issues in the framework of the analysis of the system defined by equations (1)-(3).

2 Initial Value Problem

The definition of the initial value problem (IVP) associated with the governing equations of the model requires the specification of ad hoc initial conditions. These conditions not only define the state of the system at the initial time, but also the initial drilling phase, the activation time shift and appropriate history variables. The history variables cannot be freely chosen. They must be defined such that reverse-time integration of the system from the initial conditions leads to the state defined by the history variables at their update location.

As an example, we consider the initialization of the system in the BC phase. Complete definition of the initial conditions is equivalent to specifying vector $[\theta_0 \ \bar{\theta}_0 \ \theta_P \ \tau_S]^T$ in addition to the drilling phase. The BC phase necessarily originates from a $FC \rightarrow BC$ transition point, $[\theta_p \ 0]^T$. Accordingly, the peak penetration must be initialized as a function of the initial state. Assuming that no activation takes place between the transition and initial points—this entails choosing τ_s sufficiently large—we impose the initial conditions to belong to an

arch of trajectory emanating from the associated peak penetration. Solving the equation of motion, we find

$$\theta_p\left(\theta_0,\bar{\theta}_0\right)=\begin{cases}\frac{(\gamma-1)\theta_0-\lambda_S-\sqrt{(\theta_0-\lambda_S)^2-(\gamma-2)\bar{\theta}_0^2}}{\gamma-2}, & \gamma\neq 2\\ \theta_0-\frac{\bar{\theta}_0^2}{2(\lambda_S-\theta_0)}, & \gamma=2\end{cases}. \tag{4}$$

This expression constraints the choice of the initial state, the argument of the square root having to be positive for valid conditions. In fact, a stronger constraint, defined by the $BC{\rightarrow}FF$ transition locus, can be found.

Figure 2 illustrates the dependency of the peak penetration on the initial state as well as the constraints on the choice of this state. Three initial points (A,B,C) are considered. Forward- and reverse-time integrated trajectories are shown. Similar developments can be done when choosing the initial drilling phase to be FC or FF.

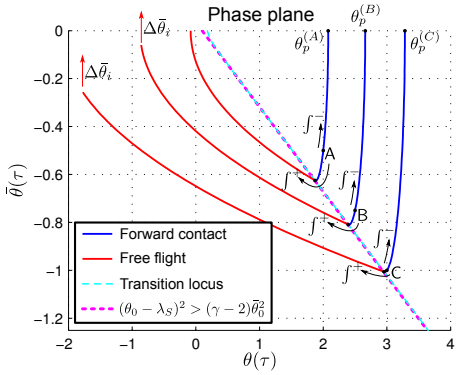

Figure 2: Dependence of the history variables on the initial conditions.

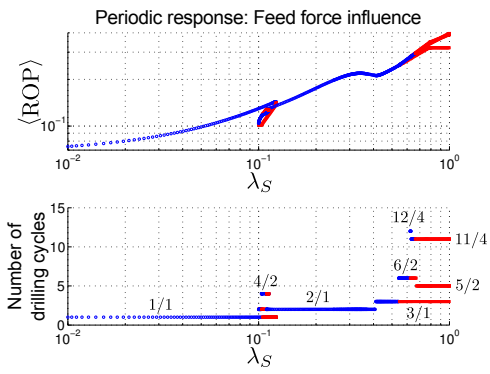

Figure 3: Average steady-state rate of penetration and number of drilling cycles as a function of the vertical thrust, $(\psi,\gamma)=(10,10)$. Blue (red) markers denote stable (unstable) solutions.

The hybrid nature of the system and the presence of history variables complicates the definition of the associated IVP. These complexities can nonetheless be circumvented by a specific choice of initial conditions: the $FC{\rightarrow}BC$ transition, i.e. $[\theta_0\ \bar{\theta}_0]^T=[\theta_p\ 0]^T$. In addition to simplifying their definition, the transition point offers the advantage that it belongs to all drilling cycles and that the trajectory is smooth in its neighborhood, facts that matter for the computation of limit cycles.

3 Computation of Limit Cycles

The computation of the average steady-state penetration rate requires the knowledge of the system steady-state response. This response, if not aperiodic, can be computed by solving the boundary value problem (BVP) defined by enforcing periodicity conditions on the system state $\mathbf{\Gamma} = [\theta \ \bar{\theta}]^T$ after one period of the limit cycle

$$\mathbf{\Gamma}(T) = [\theta_p \ 0]^T = \mathbf{\Gamma}(0), \tag{5}$$

with $T = n\psi$, the governing equations being non-autonomous. The integer factor n is the harmonic ratio.

Several techniques exist for numerically solving equation (5), see [6]. Given the hybrid nature of the system, application of the single shooting method seems most appropriate. This procedure transforms the BVP problem into an equivalent nonlinear algebraic one: find the initial conditions $[\theta_p \ \tau_s]^T$ that ensure verification of the periodicity condition after integration of the associated IVP over one period. Thus, two ingredients are required to compute the steady-state response: (i) a procedure to integrate the governing equations and (ii) a procedure to solve a nonlinear algebraic system of equations.

Time integration of the governing equations is performed using an event-driven scheme [1]. Closed-form solutions of the governing equations are used for the parametrization of the trajectory and event-detection. To solve the nonlinear system of equations resulting from the problem formulation, we have recourse to an iterative Newton-based algorithm. As this procedure requires an initial guess close enough to the solution to ensure its convergence, it has been embedded in an adaptive continuation procedure based on an arclength parametrization [6]. The latter allows continuation of solution branches in the space of the model parameters, enabling the computation of the average steady-state rate of penetration for range of parameters

$$\langle \mathrm{ROP} \rangle = \frac{1}{n\psi} \int_0^{n\psi} \bar{\theta}(s) ds. \tag{6}$$

Figure 3 shows typical results obtained from the computation of the steady-state response via the continuation procedure. On the upper graph, the average rate of penetration is plotted versus the vertical force on the tool. The bottom plot depicts the average number of drilling cycles; that is, the ratio between the number of drilling cycles m and the harmonic ratio n, where m is defined as the number of $FC \rightarrow BC$ transitions in the periodic drilling phase sequence characterizing the limit cycle. The marker color is representative of the stability

of the computed limit cycles. Blue markers denote locally stable solutions while red ones represent unstable limit cycles.

4 Computation of Floquet Multipliers

The local asymptotic stability of periodic orbits can be assessed by evaluation of the Floquet multipliers associated with the trajectory, i.e. the eigenvalues of the monodromy matrix that characterizes the growth of perturbations along the periodic orbit after one period

$$\mathbf{M}_{n\psi} = \frac{\partial \mathbf{\Gamma}_{n\psi}}{\partial \mathbf{\Gamma}_0}. \tag{7}$$

Multipliers lying within the unit circle correspond to stable solutions while those outside the reference circle are related to unstable orbits. The linear analysis is inconclusive in case several multipliers lie on the circle itself [6].

For smooth systems, the monodromy matrix is continuously defined and can be obtained by integration of the variational equation associated with the nonlinear system under study [6]. This is no longer the case when non-smooth systems are considered. The fundamental solution matrix associated with the variational problem may exhibit discontinuities at the points of non-smoothness along the periodic orbit. A measure of these jumps is the so-called saltation matrix, that is defined across the non-smooth event along the limit cycle [5].

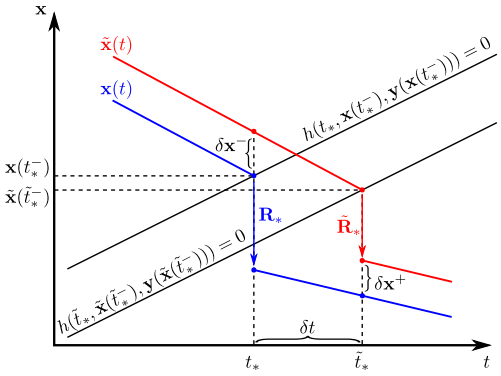

Figure 4: Jump of the state discrepancy between nearby trajectories on a transition border with reset map.

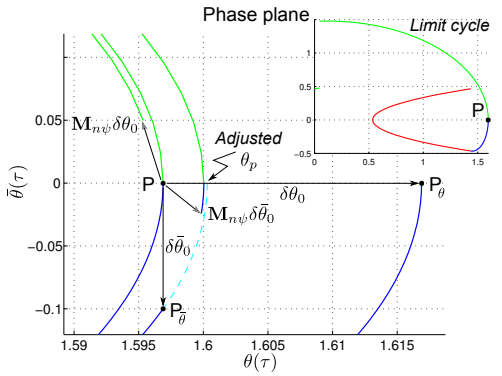

Figure 5: Reference limit cycle and perturbed trajectories for the numerical computation of the monodromy matrix, $(\lambda_S, \psi, \gamma) = (0.12, 10, 10)$.

In the next paragraphs, we derive the expression of the saltation matrix for a non-smooth event that depends on the time, the state and the history

variables. Also, a reset map, ruling state discontinuities at the non-smooth event, is considered. Figure 4 serves as support for the definition of the introduced quantities.

Let $\mathbf{x}(t) \in \mathbb{R}^n$ denote the reference trajectory of a system in the state-space and $\tilde{\mathbf{x}}(t)$ be a nearby trajectory. Let also define the non-smooth event by the scalar function $h(t, \mathbf{x}(t), \mathbf{y}(\mathbf{x}(t))) = 0$, where $\mathbf{y}(\mathbf{x}(t)) \in \mathbb{R}^m$ refers to the vector of history variables. The vector fields of the system prior to and after the transition are referenced as $\mathbf{f}_*^{\pm} = \mathbf{f}^{\pm}(t_*, \mathbf{x}(t_*^{\pm}), \mathbf{y}(\mathbf{x}(t_*^{\pm})))$, and the reset map on the transition border is given by $\mathbf{R}(\mathbf{x}(t_*))$ or $\mathbf{R}(\tilde{\mathbf{x}}(\tilde{t}_*))$. Restricting our analysis to the linearized dynamics only, all the presented developments must be understood as exact in a first-order sense.

The state discrepancies, or perturbations, before and after transition are defined as

$$\delta\mathbf{x}^- = \tilde{\mathbf{x}}(t_*^-) - \mathbf{x}(t_*^-) \qquad \text{and} \qquad \delta\mathbf{x}^+ = \tilde{\mathbf{x}}(\tilde{t}_*^+) - \mathbf{x}(\tilde{t}_*^+), \tag{8}$$

with $\tilde{t}_* = t_* + \delta t$. Accounting for the reset map relations $\tilde{\mathbf{x}}(\tilde{t}_*^+) = \mathbf{R}(\tilde{\mathbf{x}}(\tilde{t}_*^-))$ and $\mathbf{x}(t_*^+) = \mathbf{R}(\mathbf{x}(t_*^-))$ and that, to first order, we have $\tilde{\mathbf{x}}(\tilde{t}_*^-) = \mathbf{x}(t_*^-) + \delta\mathbf{x}^- + \mathbf{f}_*^- \, \delta t$ and $\tilde{\mathbf{x}}(\tilde{t}_*^+) = \mathbf{x}(t_*^+) + \mathbf{f}_*^+ \, \delta t + \delta\mathbf{x}^+$, the first-order expansion around the reference transition point reads

$$\delta\mathbf{x}^+ = \left.\frac{\partial \mathbf{R}}{\partial \mathbf{x}}\right|_{\mathbf{x}(t_*)} \left(\delta\mathbf{x}^- + \mathbf{f}_*^- \, \delta t\right) - \mathbf{f}_*^+ \, \delta t. \tag{9}$$

Expanding $h(\tilde{t}_*, \tilde{\mathbf{x}}(\tilde{t}_*^-), \mathbf{y}(\tilde{\mathbf{x}}(\tilde{t}_*^-))) = 0$ around $(t_*, \mathbf{x}(t_*^-), \mathbf{y}(\mathbf{x}(t_*^-)))$, we get δt as a function of the pre-transition perturbation δx^-

$$\delta t = -\frac{\left(\frac{\partial h}{\partial \mathbf{x}} + \frac{\partial h}{\partial \mathbf{y}}\frac{\partial \mathbf{y}}{\partial \mathbf{x}}\right)^T}{\frac{\partial h}{\partial t} + \left(\frac{\partial h}{\partial \mathbf{x}} + \frac{\partial h}{\partial \mathbf{y}}\frac{\partial \mathbf{y}}{\partial \mathbf{x}}\right)^T \mathbf{f}^-} \delta\mathbf{x}^-, \tag{10}$$

where all expressions are evaluated at the reference point. Inserting this result into the expression of the post-transition state discrepancy, we obtain the saltation matrix $\mathbf{S}$ that quantifies the jump of linear perturbations across the non-smooth event

$$\delta\mathbf{x}^+ = \underbrace{\left(\left.\frac{\partial \mathbf{R}}{\partial \mathbf{x}}\right|_{\mathbf{x}(t_*)} + \frac{\left(\mathbf{f}_*^+ - \left.\frac{\partial \mathbf{R}}{\partial \mathbf{x}}\right|_{\mathbf{x}(t_*)} \mathbf{f}_*^-\right)\left(\frac{\partial h}{\partial \mathbf{x}} + \frac{\partial h}{\partial \mathbf{y}}\frac{\partial \mathbf{y}}{\partial \mathbf{x}}\right)^T}{\frac{\partial h}{\partial t} + \left(\frac{\partial h}{\partial \mathbf{x}} + \frac{\partial h}{\partial \mathbf{y}}\frac{\partial \mathbf{y}}{\partial \mathbf{x}}\right)^T \mathbf{f}^-} \right)}_{\mathbf{S}} \delta\mathbf{x}^-. \tag{11}$$

State-dependency of the history variables should thus be accounted for in the calculation of the saltation matrix.

Application of this result to the limit cycle shown in Figure 5 permits the validation of the numerical computation of the monodromy matrix. For this limit cycle, characterized by the periodic sequence $(BC \to FF \to FC \to \Delta\bar{\theta}_i \to FC)_{\circlearrowleft}$, the matrix can be calculated both numerically and analytically. While the numerical approach relies on application of definition (7) by approximating the partial derivatives with finite differences using nearby orbits to the limit cycle, see Figure 5, the analytical one consists in decomposing the flow in smooth sections along the limit cycle and introducing the appropriate saltation matrices at non-smooth events

$$\begin{aligned}\mathbf{M}_{n\psi} = \mathbf{S}_{FC\to BC} \cdot \mathbf{\Phi}_{FC}(\tau_{FC,2}) \cdot \mathbf{S}_{\Delta\bar{\theta}_i} \cdot \mathbf{\Phi}_{FC}(\tau_{FC,1}) \ \cdots \\ \cdots \cdot \mathbf{S}_{FF\to FC} \cdot \mathbf{\Phi}_{FF}(\tau_{FF}) \cdot \mathbf{S}_{BC\to FF} \cdot \mathbf{\Phi}_{BC}(\tau_{BC}), \end{aligned} \tag{12}$$

where $\mathbf{\Phi}_{XX}(\tau_{XX})$ refers to the fundamental solution matrix of drilling phase XX that can be analytically calculated and shown to depend on the phase duration τ_{XX} only, and $\mathbf{S}_{YY}$ is the saltation matrix corresponding to non-smooth event YY.

Application of the validation procedure on different periodic sequences has provided the necessary confidence in the numerical computation procedure—that proves more versatile as it is applicable to any sequence of phases, regardless of it—to assess the periodic solutions computed via the shooting procedure. These computations have yielded the stability results shown in Figure 3.

5 Conclusions

This paper develops some specificities of the percussive drilling model proposed by Depouhon et al. [4]. In particular, it addresses the issues relative to the presence of history variables in the formulation of initial conditions and for the calculation of the saltation matrix at non-smooth events that depend on these history variables.

The main results evidence the constrained nature of the history variables when defining the initial value problem associated with the governing equations of the model as well as the dependence of the saltation matrix on the gradient of the history variables evaluated at the transition point. The former result is of critical importance for correct simulation of the system behavior and the assessment of its periodic steady-state response. The latter is an extension of the theory proposed in [3, 5].

References

[1] Vincent Acary and Bernard Brogliato. *Numerical Methods for Nonsmooth Dynamical Systems. Applications in Mechanics and Electronics.* Springer Verlag Berlin Heidelberg, 2008.

[2] Muhammad Amjad. *Control of ITH Percussive Longhole Driling in Hard Rock*. Ph.D. thesis, McGill University, Montreal, Quebec, Canada, 1996.

[3] Jan Awrejcewicz and Claude-Henri Lamarque. *Bifurcation And Chaos In Nonsmooth Mechanical Systems*. World Scientific Publishing Co., 2003.

[4] Alexandre Depouhon, Vincent Denoël, and Emmanuel Detournay. A drifting impact oscillator with periodic impulsive loading: Application to percussive drilling. *Physica D*, Submitted, 2012.

[5] Remco I. Leine and Henk Nijmeijer. *Dynamics and Bifurcations of Non-Smooth Mechanical Systems*. Springer-Verlag Berlin Heidelberg, 2004.

[6] Rüdiger Seydel. *Practical bifurcation and stability analysis*, volume 5. Springer New York Dordrecht Heidelberg London, 2009.